

Anthropogenic Impacts on the Distribution of Dissolved Nutrients at 4 Major River Mouths Discharging into the Inner Gulf of Thailand

Suparat Srisaard¹, Penjai Sompongchaiyakul^{1,*}, Tanakorn Ubonyaem¹,
Chawalit Charoenpong¹, Narainrit Chinfak² and Sujaree Bureekul^{1,3}

¹Department of Marine Science, Faculty of Science, Chulalongkorn University, Bangkok 10330, Thailand

²Department of Chemistry, School of Science, King Mongkut's Institute of Technology Ladkrabang, Bangkok 10520, Thailand

³Center of Excellence for Marine Biotechnology, Department of Marine Science, Faculty of Science, Chulalongkorn University, Bangkok 10330, Thailand

(*Corresponding author's e-mail: spenjai@hotmail.com)

Received: 7 July 2025, Revised: 7 August 2025, Accepted: 17 August 2025, Published: 17 October 2025

Abstract

Anthropogenic activities have been identified as key contributors to nutrient loading and phytoplankton blooms along the eastern coast of the Inner Gulf of Thailand (inner GoT). This study provides a comparative analysis of dissolved nutrient levels and distributions at the river mouths of 4 major basins discharging into the inner GoT in the same period: Maeklong (MK), Thachin (TC), Chaophraya (CPY), and Bangpakong (BPK). Physicochemical parameters were measured and dissolved nutrients, in inorganic and organic forms, were examined using spectrophotometric methods. The study was conducted through monthly and seasonal monitoring (dry and wet seasons) in 2019. Monthly sampling focused on spatial variation between upstream and downstream stations of each river, while additional sites (6 - 8 stations) at the river mouths were used to monitor vertical profile changes during dry and wet seasons. Results indicated that anthropogenic influences significantly affected nutrient concentrations and their spatial distribution. TC exhibited the highest average dissolved inorganic phosphorus ($9.39 \pm 4.83 \mu\text{M}$) and lowest dissolved oxygen ($1.43 \pm 1.06 \text{ mg L}^{-1}$), reflecting high domestic waste input, organic pollution, and hypoxic conditions. Exceptionally high dissolved organic nitrogen concentrations in TC ($284 \pm 62.5 \mu\text{M}$) and CPY ($304 \pm 124 \mu\text{M}$) suggested metropolitan areas as major DON sources, with the potential to enhance phytoplankton growth in the inner GoT. In BPK, dam operations altered hydrological dynamics and nutrient distribution, while MK, the least disturbed basin, showed the lowest nutrient levels. A negative correlation between nutrient concentrations and salinity, along with vertical nutrient profiles, indicated that water mixing was a dominant process controlling nutrient distribution at all river mouths. This study highlighted the anthropogenic influence and the role of nutrients especially DON in the inner GoT, providing insights into eutrophication, phytoplankton blooms, and deoxygenation - essential for sustaining fisheries and informing site-specific environmental regulations.

Keywords: Dissolved nutrient, Anthropogenic impact, Dissolved organic nitrogen (DON), River mouths, Water quality, The Inner Gulf of Thailand

Introduction

Increasing global population has intensified anthropogenic activities, leading to elevated nutrient loads at river mouths [1]. In South and Southeast Asia, rapid urbanization and economic development have

driven the expansion of domestic wastewater discharge and agricultural land [2,3]. Essential macronutrients - dissolved silicate (DSi), nitrogen (N), and phosphorus (P), in both organic and inorganic forms - support phytoplankton growth [4]. A range of anthropogenic

activities, including land-use change, infrastructure development, and agriculture, alter nutrient concentrations and their spatial distribution [5]. In densely populated regions, domestic wastewater enhances dissolved inorganic phosphorus (DIP), dissolved inorganic nitrogen (DIN), dissolved organic nitrogen (DON), and phosphorus (DOP) levels [6,7]. Consequently, anthropogenic inputs are fundamentally linked to nutrient variability in river systems.

Estuaries and river mouths serve as critical conduits for transporting terrestrial nutrients to coastal waters [8]. Elevated nutrient inputs often lead to phytoplankton blooms and shifts in community structure [9]. For instance, the Pearl River Estuary in China has experienced eutrophication and increased phytoplankton productivity due to urban and agricultural nutrient loading [10]. Similarly, studies in Jiaozhou Bay highlight the role of bioavailable DON in fueling coastal algal communities.

In Thailand, 4 major river mouths - MaeKlong (MK), Thachin (TC), Chaopraya (CPY), and Bangpakong (BPK) - discharge anthropogenic nutrients (especially DIP and DIN) into the inner Gulf of Thailand (inner GoT), fueling eutrophication and phytoplankton blooms reported since 1957 [11,12]. These blooms have led to ecological imbalance, fish kills, aquaculture losses, and economic impacts on tourism and fisheries [11,13,14]. For instance, organic matter from blooms can cause hypoxia and harming marine life. Between 1981 - 1995, fish kills linked to harmful algal blooms (HABs) occurred annually or biannually. Although less frequent between 2000 - 2017, a major 2023 bloom of *Noctiluca scintillans* in Chonburi caused hypoxia and mussel mortality, with reported losses of USD 14,000 [14-16]. Similar events have caused damages USD 6 and 8.5 million in Malaysia and the Philippines, respectively [14].

Despite long-standing recognition of eutrophication, baseline data on nutrient inputs remain limited. Recent studies [17,18] confirm persistent anthropogenic nutrient loading, but key knowledge gaps remain. Most previous research relied on seasonal sampling (dry/wet monsoons), overlooking potential non-seasonal nutrient fluctuations [19-21], and often neglected dissolved organic nutrients (DOP and DON), which significantly influence phytoplankton growth and hypoxia [22]. Moreover, studies typically focused on

single rivers, limiting cross-system comparisons critical for regional management. To address these gaps, we conducted monthly and seasonal sampling across all 4 river mouths in 2019. Our objectives were to (1) compare spatial and seasonal variations of physicochemical parameters and both inorganic and organic nutrients, and (2) examine nutrient distribution patterns linked to anthropogenic sources. Sampling included vertical salinity and nutrient profiles to assess estuarine mixing. This is among the first studies to provide a year-round comparative assessment of nutrient inputs across all 4 major Thai river systems discharging into the inner GoT. Thus, understanding the characteristics of these nutrients may help mitigate phytoplankton blooms and associated fishery losses in the inner GoT.

Materials and methods

Study area

The Gulf of Thailand (GoT), a shallow inlet of the South China Sea, is an ecologically and economically important semi-enclosed sea in Southeast Asia. Its inner region (~100×100 km², ~15 m average depth) receives discharge from 4 major rivers: MK, TC, CPY and BPK, across latitudes 13° 19' 12" N - 13° 45' 36" N and longitudes 99° 55' 12" E - 101° 05' 59" E. According to discharge data from 2014 - 2018 provided by the Royal Irrigation Department (RID), which supported the experimental design, the MK River basin is forested upstream and increasingly populated downstream, regulated by major dams, with an average discharge of 125×10⁶ m³ day⁻¹ [23-25]. The TC and CPY basins lie in the Chao Phraya Plain, dominated by agriculture and agro-industries; CPY has more intensive land use and urbanization, especially near Bangkok, and a much higher discharge (401×10⁶ m³ day⁻¹) than TC (4.83×10⁶ m³ day⁻¹) [23,24]. The BPK River, formed by the Prachin Buri and Nakhon Nayok Rivers, has diverse land use (paddy, forest, crops, eucalyptus) and faces seawater intrusion up to 52 km inland [23,26-28]. All basins are shaped by the Southeast Asian monsoon, with dry-season winds (mid-October to mid-February) and wet-season rainfall (mid-May to mid-October) driving strong seasonal variation in river discharge. In 2019, discharges during the dry/wet seasons were, respectively, 2,290/11,955 (MK), 119/1,237 (TC),

80/1,700 (CPY), and 701/7,935 MCM (BPK), based on data from RID stations [24-26].

The 4 river basins are strongly influenced by the Southeast Asian summer monsoon. During the dry season, northeasterly winds bring cool, dry air from Mongolia and China, while the wet season is driven by moist southwesterly winds from the Indian Ocean, resulting in heavy rainfall and cloud cover [26]. In 2019,

average dry-season discharges for the MK, TC, CPY, and BPK rivers were 2,290, 119, 80, and 701 million cubic meters (MCM), increasing to 11,955, 1,237, 1,700, and 7,935 MCM during the wet season [24]. Discharge data were obtained from RID stations: K.11A (MK), Pholarthep Water Gate (TC), C.13 (CPY), and Ny.1B and Kgt.3 (BPK) [24].

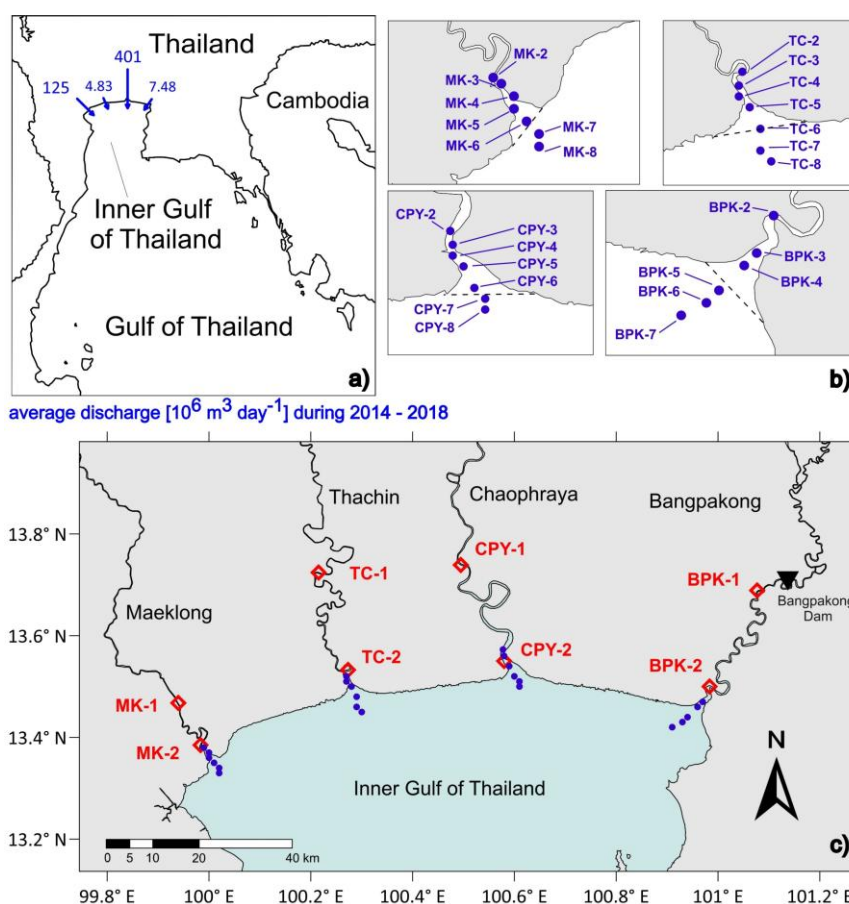


Figure 1 Map of 4 major rivers flowing into the inner Gulf of Thailand (inner GoT); Maeklong (MK), Tachin (TC), Chaophraya (CPY), and Bangpakong (BPK). The maps show (a) average discharge [$10^6 \text{ m}^3 \text{ day}^{-1}$] during 2014 - 2018, (b) the close-up seasonal stations, and (c) the sampling stations. The red diamond points and blue round dot in (c) shows monthly and seasonal sampling stations, respectively.

Sample collection

Surface water samples (0.5 m depth) were collected monthly from January to December 2019 at sites marked in **Figure 1(b)**. Each river - MK, TC, CPY, and BPK - had 2 fixed stations: upstream (MK-1, TC-1, CPY-1 and BPK-1) located 24.9 - 60.6 km from the coast, and downstream (MK-2, TC-2, CPY-2 and BPK-2) located 3.04 - 8.13 km from the coast. Additional

seasonal sampling was conducted during the dry (30 May - 14 June) and wet (25 October - 9 November) seasons of 2019 at 6 - 8 sites along each river's salinity gradient near the mouth, coinciding with neap tides to limit seawater intrusion. Vertical sampling was performed based on depth (measured using a HONDEX[®] PS-7): 1 near-bottom sample for depths ≤ 4

m; mid- and bottom samples for 5 - 10 m; and 3 layers for depths ≥ 10 m.

All sampling tools were acid-cleaned (10% HCl), rinsed with distilled water, and neutralized. Water samples were collected using a 2-L PTFE sampler and stored in pre-rinsed 1-L LDPE Nalgene® bottles at 4 °C until filtration. Filtration used pre-combusted (500 °C, 5 h), pre-weighed GF/F filters; filters were dried (60 °C, 5 h), stored in desiccators, and reweighed for suspended particulate matter (SPM) determination. Filtrates were used to rinse and fill 2 50-mL LDPE bottles: 1 for immediate analysis of dissolved inorganic silicate (DSi), phosphate (DIP), and nitrogen species (NO_3^- , NO_2^- , and NH_4^+), and 1 frozen at -20 °C for later analysis of dissolved organic phosphorus (DOP) and nitrogen (DON).

Physicochemical characteristic

The *in situ* physicochemical characteristics of the water at the sampling sites were measured using a YSI 650 Multiparameter Display System (650 MDS). Parameters measured included salinity, dissolved oxygen (DO), pH, and temperature (Tables S1 and S2).

Chemical analysis

Dissolved inorganic nutrients (DSi, DIP, NO_3^- , NO_2^- and NH_4^+) were analyzed using spectrophotometric methods based on Strickland and Parsons (1972), a protocol still widely applied in recent studies [27,29]. Dissolved organic phosphorus (DOP) and nitrogen (DON) were calculated by subtracting their respective inorganic concentrations from total dissolved phosphorus (TDP) and total dissolved nitrogen (TDN). TDP and TDN were measured from defrosted samples digested with acidic potassium persulfate, followed by spectrophotometric analysis in accordance with Strickland and Parsons [30] and Grasshoff, Kremling [31]. The accuracy of the experiment was determined using Relative Percent Difference (%RPD). %RPD for DSi, DIP, TDP, TDN, NO_3^- , NO_2^- , and NH_4^+ were 1.72%, 1.99%, 3.76%, 4.64%, 4.51%, 3.94%, and 7.94%, respectively. The detection limits were 0.572,

0.965, 0.806, 21.2, and 0.301 μM , respectively. In addition, to ensure data quality and assess analytical precision, both blank and reagent tests were conducted throughout the sampling and laboratory analysis processes. Procedural blanks were included for each nutrient analysis batch to detect any background contamination. Reagent blanks were used to account for potential interferences from chemicals and instruments.

Data analysis

The sampling map shown in this study was plotted using Surfer® 16.0.330, a software for 3D data visualization and mapping. Statistical graphs were plotted using Grapher® 15.0.259. Vertical profiles of the water column were visualized using Ocean Data View® 5.1.7.

Statistical analysis

Pearson's 2-tailed correlation analysis was applied to evaluate the relationships among physicochemical parameters and nutrient concentrations. Correlations were considered statistically significant at the 95% ($p < 0.05$) and 99% ($p < 0.01$) confidence levels. All statistical analyses were conducted using IBM SPSS® Statistics software version 29.0.0.0 (241).

Results and discussion

Estuarine classification in the inner GoT

Vertical salinity profiles revealed distinct estuarine mixing patterns across the 4 river mouths [32]. MK showed persistent stratification with strong bottom-layer seawater intrusion (Figure 2), attributed to its high discharge, while TC and BPK were well-mixed due to low flow. CPY exhibited partial mixing, consistent with its moderate discharge. Salinity generally declined in the wet season, except at TC, where seawater intrusion extended further inland. TC, a tributary of CPY, had discharges of 119 and 1,237 MCM during the dry and wet seasons, respectively [25]. BPK, affected by dam regulation, had elevated salinity due to limited freshwater input.

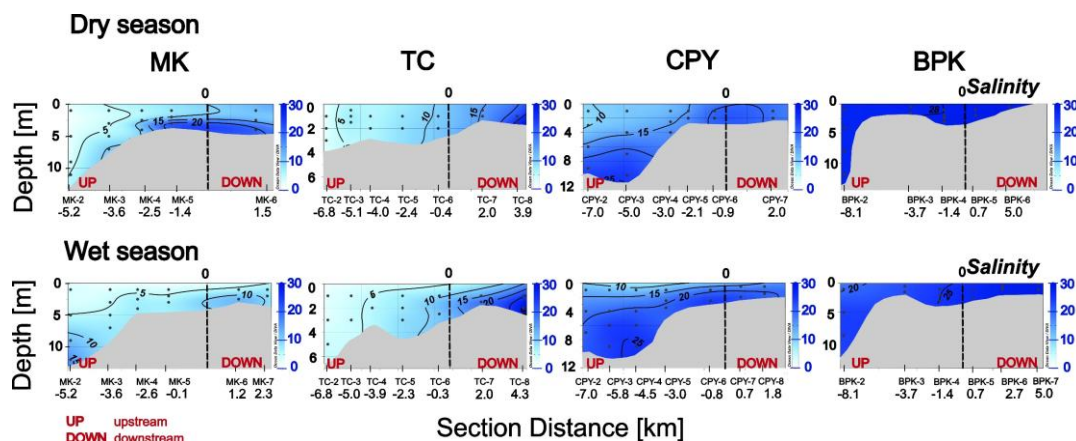


Figure 2 Vertical salinity profiles during the dry and wet seasons. Each sub-figure includes a vertical dashed line at 0 km, marking the coastline at the river mouth. “UP” and “DOWN” indicate the landward and seaward directions, respectively.

Influence of water mixing on nutrient distribution at the river mouths

The distributions of DSi, DIP, DIN, and DON across the study area showed complex spatial and seasonal patterns. An in-depth description of each nutrient’s distribution is provided in the **Supplementary Section 2**. However, it was clear that water mixing also played a key role in nutrient dynamics. Most nutrient concentrations followed the salinity gradient, with higher levels in freshwater and a gradual decrease toward seawater due to dilution (**Figures S3** and **S4**). In addition, a significant negative Pearson’s correlation between nutrient concentrations and salinity (**Tables S4** and **S5**) - commonly observed at all river mouths - indicated the diluting effect and water mixing influence of seawater [33,34].

Comparison of anthropogenic impact on nutrient distribution from 4 main river mouths

The spatial and temporal distribution of nutrient concentrations exhibited considerable variability across the 4 main rivers (**Figure 3**). DSi in the main rivers ranged from 5.53 - 270 μM . Among rivers, the TC exhibited the highest average DSi concentration at both upstream ($205 \pm 51.0 \mu\text{M}$) and downstream stations ($177 \pm 66.6 \mu\text{M}$). Notably, TC basin presented distinct patterns, with DIP concentrations showing a significant increase from upstream ($4.34 \pm 0.77 \mu\text{M}$) to downstream ($11.0 \pm 5.74 \mu\text{M}$). Furthermore, the highest NH_4^+ concentration ($55.0 \pm 50.1 \mu\text{M}$) was observed at the

downstream station of the TC river (TC-2), contrasting with upstream concentrations that were roughly half. Concurrently, CPY River recorded the highest average NO_2^- concentration ($\sim 30 \mu\text{M}$) among all rivers, and its DON average was twice as high upstream (CPY-1) as downstream (CPY-2), a pattern differing from its DIN levels which remained similar between upstream and downstream.

Each river basin exhibited distinct characteristics. A comprehensive comparison, supported by statistical analysis, is presented in the following sections.

MK river basin

Forest cover and water mixing were the primary factors influencing nutrient distribution in the MK Basin. Forests, particularly in tropical regions, play a crucial role in regulating dissolved inorganic nutrients. For instance, a study in southeastern Brazil found that forested watersheds exhibited significantly lower pollutant levels compared to those dominated by agricultural land use [35]. In the MK Basin, much of the area is covered by evergreen forest and protected areas, including Khao Laem and Erawan National Parks [23]. Consequently, concentrations of nutrients (DIP, DIN, DOP, and DON) were generally low, with the exception of DSi. Pearson’s correlation analysis based on monthly data (**Table S3**) revealed a moderate positive correlation (~ 0.5 , $p < 0.01$) between DSi and DIN (including NO_2^- and NO_3^-), suggesting a common freshwater origin for both nutrient types [36].

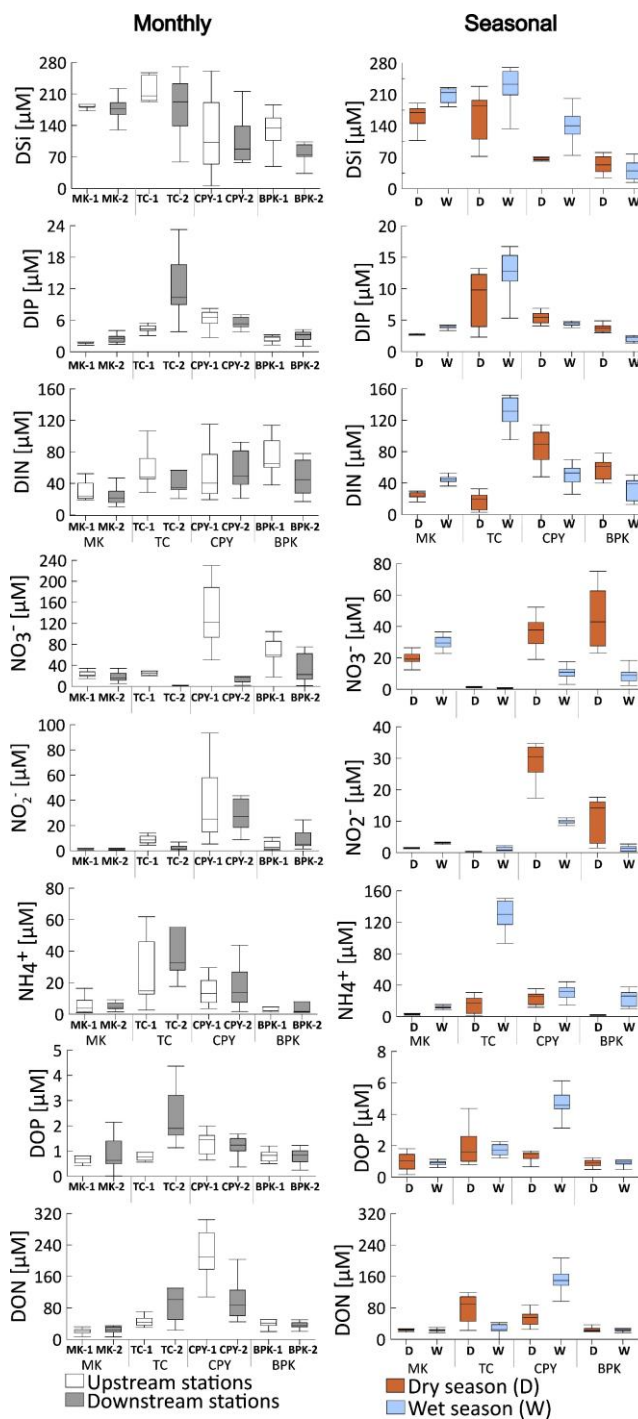


Figure 3 Box plots of nutrient concentrations across the 4 river basins, categorized by monthly (upstream-downstream stations) and seasonal (dry-wet season) variations.

TC river basin

Intensive anthropogenic land use, hypoxia, and limited water mixing are key factors contributing to elevated nutrient concentrations in the TC Basin. Swine farms, agriculture, and urban areas likely drive high inputs of both inorganic and organic nutrients [37,38]. The shift in land use - from fisheries to industrial zones (1982 - 2010) and tourism development post-2015 -

aligns with national economic plans prioritizing industrial growth [39], contributing to long-term water quality degradation. The TC River is now classified as having “poor” water quality [40].

Our results showed elevated DIP concentrations and low DO levels, especially in bottom waters - conditions indicative of hypoxia. Under these oxygen-deficient conditions, microbial processes such as

ammonification and dissimilatory nitrate reduction likely promote hydrogen sulfide formation and DIP release from SPM [41]. Elevated DOP and DON further contribute to oxygen depletion via microbial decomposition, supported by previously reported high BOD values in the river's midsection [40,42].

The highest DIP levels occurred downstream, likely reflecting cumulative impacts of non-point source pollution. Agricultural runoff, urban sewage, and industrial effluents are major contributors [43,44], with fertilizers and phosphorus loss from paddy fields playing a substantial role [45-47]. The dense population and intense aquaculture and industrial activity around station TC-2, especially in Samut Sakhon Province, further underscore the anthropogenic pressures driving phosphorus enrichment [23,48]. Pearson's correlation analysis based on monthly data (**Table S3**) also revealed a strong positive correlation ($0.765, p < 0.01$) between DIP and DON, suggesting a common origin possibly linked to anthropogenic sources [43,49].

CPY River Basin

Urbanization, agriculture, and biological processes strongly shaped nutrient distributions in the CPY River. Dissolved nutrients such as DIP, NO_3^- , NH_4^+ , and DON are largely derived from urban wastewater inputs, reflecting inadequate sewage infrastructure and leakage [7,50,51]. Elevated NO_3^- and NH_4^+ concentrations likely result from DON mineralization and ammonification [50,52], consistent with previous findings that domestic sewage dominates nutrient loading in this basin [53]. In this study, the highest concentrations of NO_3^- , NO_2^- , and DON were observed at site CPY-1 in Bangkok, highlighting the impact of dense urban activity. Pearson's correlation analysis based on monthly data (**Table S3**) also revealed a moderate positive correlation ($\sim 0.5, p < 0.01$) between DIP and DIN (including NO_2^- and DON), suggesting a common origin possibly linked to anthropogenic sources [36,54].

Agricultural runoff further contributed to nutrient enrichment. Extensive rice cultivation in the CPY basin is a key source of NH_4^+ and NO_3^- , as fertilizer application significantly increases their concentrations in surface waters [38,55,56]. These findings underscore the combined influence of urban and agricultural sources in driving elevated nutrient loads. In addition to

external inputs, biological processes may enhance nitrogen availability. The prevalence of NO_3^- and NO_2^- suggests active nitrogen fixation by cyanobacteria and phytoplankton, particularly where regenerated nitrogen (NH_4^+) is limited - contrasting with conditions observed in the TC system.

BPK River Basin

Seawater intrusion, dam regulation, and water mixing at the river mouth were the primary factors influencing nutrient distribution in the BPK River. In tropical regions, seawater intrusion is typically driven by sea-level rise, cyclones, storm surges, and reduced freshwater discharge due to anthropogenic activities [57]. Such intrusion can degrade drinking water quality and reduce agricultural productivity [58]. The BPK River Basin had experienced these challenges, prompting the Thai government to construct the Bang Pakong Dam, which began operation on 6 January 2000, to limit seawater intrusion [59]. Pearson's correlation analysis based on monthly data (**Table S3**) showed no strong correlation between different nutrients types as appeared in other rivers. This could supported various nutrients origin influenced by seawater intrusion.

However, dam operation had altered hydrological dynamics, reduced river discharge and causing several issues at the river mouth: (1) increased tidal fluctuations and severe bank erosion, (2) accumulation of anthropogenic effluents upstream, and (3) decreased seawater availability for upstream aquaculture [59]. Consequently, nutrient distribution in the estuarine zone was heavily influenced by dam regulation.

DON loading from metropolitan into the inner GoT

Metropolitan stations (TC and CPY) were as potentially significant sources of DON to the inner GoT. DON is derived from both natural and anthropogenic sources and often dominates the TDN pool in various ecosystems [60]. For instance, studies have reported that DON comprises over 70% of TDN in South American forests [61], 40% - 90% in southeastern USA watersheds [62] and 75% - 83% in northern Thai forests, indicating a substantial natural contribution [63]. However, anthropogenic activities also play a major role in DON loading globally. Intensive agriculture, particularly with high fertilizer usage, has been shown

to elevate fluvial DON concentrations, often with more reactive forms [49]. In northern Thailand, industrial and agricultural activities were also identified as DON sources [64]. Urban infrastructure, including aging sewer systems, can further contribute to DON leakage [7].

Evidence from highly urbanized areas supports this link between human activity and DON contamination. For example, a study in São Paulo, Brazil, found DON loads positively correlated with population density [65]. Similarly, during the COVID-19 pandemic, excessive disinfectant use in Wuhan was associated with elevated DON concentrations in surface waters [66], suggesting that even routine urban chemical use may contribute to DON pollution. Thus, DON observed at TC and CPY likely originates from a combination of natural processes and anthropogenic inputs, including agriculture, industry, and urban infrastructure.

Although often overlooked, DON can play a significant role in stimulating phytoplankton growth in coastal ecosystems. Historically, DON was excluded as a major nutrient source due to assumptions of low bioavailability, particularly in temperate regions [67]. However, several studies have shown that bioactive DON can be rapidly mineralized into inorganic forms, becoming readily available to phytoplankton [67,68]. DON has been implicated in promoting phytoplankton growth and blooms in coastal waters [22]. For example, brown tide events in Long Island, USA, were linked to elevated DON levels [69]. Additionally, dinoflagellates have demonstrated a preference for DON uptake, contributing to bloom formation [70,71].

Phytoplankton blooms in the inner GoT reflected persistent nutrient imbalances, with 97 events recorded between 1957 and 2001 [11]. *Noctiluca scintillans* and *Trichodesmium erythraeum* dominate these blooms. MODIS data (2003 - 2017) show chlorophyll-a concentrations closely tied to discharges from the TC and CPY rivers, indicating urban nutrient sources [72]. High DSi, DIP, and DIN levels enhance diatom prey, indirectly fueling *N. scintillans* blooms [73,74], particularly near TC [15], where blooms are linked to hypoxia and fish kills [14].

Effective nutrient management must consider all dissolved forms, particularly DON. The Coordinating Body on the Seas of East Asia (COBSEA) is one of the

key international organizations addressing marine pollution and nutrient management. According to the “Strategic Directions 2023 - 2027,” anthropogenic pollution remains a priority under the Regional Seas Strategic Direction 2022 - 2025. Enhancing nutrient runoff data is essential to support evidence-based and sustainable coastal management [75].

Conclusions

This study presents a comprehensive comparison of 4 major watersheds discharging nutrients into the inner GoT during a synchronized sampling period. The results confirmed that anthropogenic activities and water mixing are key drivers of dissolved nutrient distributions at river mouths. The MK Basin, the most pristine site, showed the lowest concentrations of DIP, DIN, DOP, and DON, highlighting the critical role of forested areas in regulating nutrient loads. In contrast, TC, characterized by intensive domestic and industrial activity, exhibited the highest DIP concentrations and the lowest DO levels, indicating substantial organic pollution and possible hypoxia-induced DIP release from sediments. CPY, with similar land use to TC, showed a different DIN composition dominated by NO_3^- and NO_2^- , likely due to intensive paddy cultivation, wastewater discharge, DON remineralization, and elevated nitrogen fixation. Exceptionally high DON concentrations in TC and CPY suggested a significant, underrecognized nitrogen source from metropolitan areas to the inner GoT, potentially fueling episodic phytoplankton blooms along the eastern coast. Nutrient distribution in BPK was notably influenced by dam regulation. The Bang Pakong Dam, built to limit seawater intrusion, altered tidal dynamics, and trapped upstream domestic waste, resulting in a non-uniform nutrient pattern. Across all sites, nutrient concentrations showed strong negative correlations with salinity, and vertical profiles revealed decreasing nutrient levels with increasing seawater influence - both indicating estuarine mixing as the dominant process at the river mouths. Future nutrient policies must address all dissolved forms, especially DON, as drivers of coastal eutrophication. Regional efforts like COBSEA’s 2023 - 2027 strategy highlight marine pollution, underscoring the need for robust runoff data to inform sustainable management.

Acknowledgements

This study was supported by “The 100th Anniversary Chulalongkorn University Fund, Thailand for Doctoral Scholarship” and “The 90th Anniversary of Chulalongkorn University Fund (Ratchadaphiseksomphot Endowment Fund).

Declaration of Generative AI in Scientific Writing

Generative AI tools (e.g., ChatGPT by OpenAI) were used solely to improve the readability and language of the manuscript. All contents (graphical abstracts, graphs, maps, contour profile) was created and verified by the authors, who take full responsibility for its accuracy and integrity. No AI tools were used for data analysis, interpretation, or scientific conclusions. The tools were not listed as authors or co-authors.

CRedit author statement

Suparat Srisaard: Conceptualization, Writing - original draft, Data collection, Data curation, Methodology, Visualization, Formal analysis, Investigation. **Penjai Sompongchaiyakul:** Conceptualization, Supervision, Data curation, Writing - reviewing and editing, Funding acquisition. **Tanakorn Ubonyaem:** Field sampling, Formal analysis, Writing - reviewing and editing. **Chawalit Charoenpong:** Writing - reviewing and editing, Data curation. **Narainrit Chinfak:** Conceptualization, Supervision, Writing - reviewing and editing, Data collection. **Sujaree Bureekul:** Conceptualization, Supervision, Data curation, Writing - reviewing and editing.

References

- [1] HJ Qu and C Kroeze. Past and future trends in nutrients export by rivers to the coastal waters of China. *Science of The Total Environment* 2010; **408(9)**, 2075-2086.
- [2] A Singh. A review of wastewater irrigation: Environmental implications. *Resources, Conservation and Recycling* 2021; **168**, 105454.
- [3] CO Rusănescu, R Marin and GA Constantin. Wastewater management in agriculture. *Water* 2022; **14(21)**, 3351.
- [4] D Bandyopadhyay and H Biswas. Impacts of variable nutrient stoichiometry (N, Si and P) on a coastal phytoplankton community from the SW Bay of Bengal, India. *European Journal of Phycology* 2021; **56(3)**, 273-288.
- [5] M Delkash, FAM Al-Faraj and M Scholz. Impacts of anthropogenic land use changes on nutrient concentrations in surface waterbodies: A review. *CLEAN - Soil, Air, Water* 2018; **46(5)**, 1800051.
- [6] MA Álvarez-Vázquez, R Prego, N Ospina-Alvarez, M Caetano, P Bernárdez, M Doval, AV Filgueiras and C Vale. Anthropogenic changes in the fluxes to estuaries: Wastewater discharges compared with river loads in small rias. *Estuarine, Coastal and Shelf Science* 2016; **179**, 112-123.
- [7] WH McDowell, WG McDowell, JD Potter and A Ramírez. Nutrient export and elemental stoichiometry in an urban tropical river. *Ecological Applications* 2019; **29(2)**, e01839.
- [8] YY Hao, ZY Zhu, FT Fang, T Novak, M Čanković, E Hrustić, Z Ljubešić, M Li, JZ Du, RF Zhang and B Gašparović. Tracing nutrients and organic matter changes in Eutrophic Wenchang (China) and Oligotrophic Krka (Croatia) estuaries: A comparative study. *Frontiers in Marine Science* 2021; **8**, 663601.
- [9] R Yang, S Chen, X Zhang, R Su, C Zhang, S Liang, X Han, X Wang and K Li. Influences of the hydrophilic components of two anthropogenic dissolved organic nitrogen groups on phytoplankton growth in Jiaozhou Bay, China. *Marine Pollution Bulletin* 2021; **169**, 112551.
- [10] W Tao, L Niu, Y Dong, T Fu and Q Lou. Nutrient pollution and its dynamic source-sink pattern in the pearl river estuary (South China). *Frontiers in Marine Science* 2021; **8**, 713907
- [11] N Somsap, N Gajasen and A Piumsomboon. Physico-chemical factors influencing blooms of *Chaetoceros* spp. and *Ceratium furca* in the Inner Gulf of Thailand. *Agriculture and Natural Resources* 2015; **49**, 200-210.
- [12] S Yuenyong, A Buranapratheprat, P Thaipichitburapa, V Gunbua, P Intacharoen and A Morimoto. Fluxes of dissolved nutrients and total suspended solids from the Bang Pakong River Mouth into the Upper Gulf of Thailand. *Journal of Fisheries & Environment* 2023; **47(3)**, 68-83.
- [13] M Dai, Y Zhao, F Chai, M Chen, N Chen, Y Chen, D Cheng, J Gan, D Guan and Y Hong. Persistent

- eutrophication and hypoxia in the coastal ocean. *Cambridge Prisms: Coastal Futures* 2023; **1**, e19.
- [14] ML San Diego-McGlone, AT Yñiguez, G Benico, WM Lum, KS Hii, SC Leong, CP Leaw, M Iwataki and PT Lim. Fish kills related to harmful algal bloom events in Southeast Asia. *Sustainability* 2024; **16(23)**, 10521.
- [15] T Suwanlertcharoen, S Lawawirojwong and K Deeudomchan. Spatiotemporal distribution and occurrence of surface phytoplankton blooms using spectral indices derived from sentinel-2 imagery in the Upper Gulf of Thailand. *In: Proceedings of the Asian Conference on Remote Sensing, Colombo, Sri Lanka*. 2024.
- [16] Reuters. *Severe plankton bloom off Thailand creates marine 'dead zone'*. Guardian, London, 2023.
- [17] A Bridhikitti, M Pumkaew, T Prabamroong, GA Yu and G Liu. Processes governing nutrient dynamics in tropical urban-agriculture rivers, NE Thailand. *Sustainable Water Resources Management* 2022; **8(5)**, 156.
- [18] K Khongmanont. 2023, Effects of tidal variations on nutrient dynamics in the Chao Phraya River Estuarine Ecosystem. Master Thesis. Chulalongkorn University, Bangkok, Thailand.
- [19] B Thongdonphum and S Meksumpun. Assessment of pollution carrying capacity in the lower part of Mea Klong River, Thailand. *International Journal of GEOMATE* 2020; **19(71)**, 84-89.
- [20] G Huang, H Xue, H Liu, C Ekkawatpanit and T Sukhapunnapha. Duality of seasonal effect and river bend in relation to water quality in the Chao Phraya River. *Water* 2019; **11(4)**, 656.
- [21] X Guo, X Yan, H Bao, J Wu and S Kao. Differential response of nutrients to seasonal hydrological changes and a rain event in a subtropical watershed, Southeast China. *Water* 2022; **14(5)**, 834.
- [22] RM Kudela, JQ Lane and WP Cochlan. The potential role of anthropogenically derived nitrogen in the growth of harmful algae in California, USA. *Harmful Algae* 2008; **8(1)**, 103-110.
- [23] Land Development Department. Catalog data of Land Development Department, Available at: <http://sql.ldd.go.th/ldddata/mapsoilB1.html?fbclid=IwAR0waNp3aBWs3ejc8LRxzuJSIYHIXe-Alq2CreqHKEYB6G4iJOoGH2MQQ> Y, accessed April 2025.
- [24] Royal Irrigation Department. *Discharge in cubic metre per second during water year 2014 to 2018*. Hydrology Division, Royal Irrigation Department, Bangkok, Thailand, 2019.
- [25] Office of the National Water Resources. *The 22 river basin in Thailand and decree 2021 (in Thai)*. Office of the National Water Resources, Bangkok, Thailand, 2021.
- [26] Monsoon. Available at: <https://tmd.go.th/info/%E0%B8%A5%E0%B8%A1%E0%B8%A1%E0%B8%A3%E0%B8%AA%E0%B8%A1>, accessed April 2025.
- [27] S Yuenyong, N Nimsuwan, A Buranapratheprat and V Gunboa. Water quality of the Bangpakong River during 2016-2018. *Burapha Science Journal* 2019; **24(1)**, 138-155.
- [28] S Wongsas and S Sueathung. Effects of dam construction on salinity and water resources in lower Bang Pakong Basin. *In: Proceedings of the 28th National Convention on Civil Engineering, Phuket, Thailand*. 2023.
- [29] N Chinfak, P Sompongchaiyakul, C Charoenpong, Y Wu, J Du, S Jiang and J Zhang. Riverine and submarine groundwater nutrients fuel high primary production in a tropical bay. *Science of The Total Environment* 2023; **877**, 162896.
- [30] JDH Strickland and TR Parsons. *Part II. Inorganic micronutrients in sea water*. *In: JC Stevenson and TR Parsons (Eds.). A practical handbook of seawater analysis*. Supply and Services, Ottawa, Canada, 1972, p. 45-89.
- [31] K Grasshoff, K Kremling and M Ehrhardt. *Methods of seawater analysis*. Wiley-VCH, Weinheim, Germany, 1999.
- [32] KR Dyer. *Estuarine flow interaction with topography lateral and longitudinal effects*. *In: BJ Neilson, A Kuo and J Brubaker (Eds.). Estuarine circulation*. Humana Press, Totowa, United States, 1989, p. 39-59.
- [33] SF Dan, SM Liu, EC Udoh and S Ding. Nutrient biogeochemistry in the Cross River estuary system and adjacent Gulf of Guinea, South East Nigeria

- (West Africa). *Continental Shelf Research* 2019; **179**, 1-17.
- [34] C Xu, SF Dan, B Yang, D Lu, Z Kang, H Huang, J Zhou and Z Ning. Biogeochemistry of dissolved and particulate phosphorus speciation in the Maowei Sea, northern Beibu Gulf. *Journal of Hydrology* 2021; **593**, 125822.
- [35] K Mello, RA Valente, TO Randhir and CA Vettorazzi. Impacts of tropical forest cover on water quality in agricultural watersheds in southeastern Brazil. *Ecological Indicators* 2018; **93**, 1293-1301.
- [36] R Li, J Xu, X Li, Z Shi and PJ Harrison. Spatiotemporal variability in phosphorus species in the pearl river estuary: Influence of the river discharge. *Scientific Reports* 2017; **7(1)**, 13649.
- [37] D Zhang, X Wang and Z Zhou. Impacts of small-scale industrialized swine farming on local soil, water and crop qualities in a hilly red soil region of subtropical China. *International Journal of Environmental Research and Public Health* 2017; **14(12)**, 1524.
- [38] NVC Ngan, HV Thao and ND Giang Nam. Nutrient dynamics in water and soil under conventional rice cultivation in the Vietnamese Mekong Delta. *F1000Research* 2023; **10**, 1145.
- [39] C Thawanaphong. 2017, Morphological transformation of communities and fishery industries in Tha Chin riverfront area, Tha Chalom sub-district Mahachai sub-district and Krokkrak sub-district, Samutsakorn province. Master Thesis. Chulalongkorn University, Bangkok, Thailand.
- [40] S Nawagawong, C Chitmanat, P Chaibu and S Aroonsrimorakot. The guidelines for water quality management on the middle of Tha Chin River. *Health Science Journal of Thailand* 2024; **6(4)**, 26-33.
- [41] B Sundby, C Gobeil, N Silverberg and M Alfonso. The phosphorus cycle in coastal marine sediments. *Limnology and Oceanography* 1992; **37(6)**, 1129-1145.
- [42] D Alfrianti and A Sudradjat. Managing organic pollutant loads in the Lower Cileungsi River, Indonesia. *Water Policy* 2024; **26(10)**, 959-977.
- [43] MJ Bowes, HP Jarvie, SJ Halliday, RA Skeffington, AJ Wade, M Loewenthal, E Gozzard, JR Newman and EJ Palmer-Felgate. Characterising phosphorus and nitrate inputs to a rural river using high-frequency concentration - flow relationships. *Science of The Total Environment* 2015; **511**, 608-620.
- [44] SM Liu, RH Li, GL Zhang, DR Wang, JZ Du, LS Herbeck, J Zhang and JL Ren. The impact of anthropogenic activities on nutrient dynamics in the tropical Wenchanghe and Wenjiaohe Estuary and Lagoon system in East Hainan, China. *Marine Chemistry* 2011; **125(1)**, 49-68.
- [45] Department Pollution Control. *The status of paddy field pollution and management*. Department Pollution Control, Bangkok, Thailand, 2011.
- [46] A Khruakham, B Anurugsa and N Hungspreug. Influence of chemical fertilizer applications on water quality in paddy fields in Nong Harn, Sakon Nakhon Province, Thailand. *Agriculture and Natural Resources* 2015; **49(6)**, 868-879.
- [47] N Prathumchai, S Polprasert and C Polprasert. Evaluation of phosphorus flows in agricultural sector of Thailand. *GMSARN International Journal* 2016; **10**, 163-170.
- [48] M Schaffner, HP Bader and R Scheidegger. Modeling the contribution of point sources and non-point sources to Thachin River water pollution. *Science of The Total Environment* 2009; **407(17)**, 4902-4915.
- [49] D Graeber, IG Boëchat, F Encina-Montoya, C Esse, J Gelbrecht, G Goyenola, B Gücker, M Heinz, B Kronvang, M Meerhoff, J Nimptsch, MT Pusch, RC Silva, D von Schiller and E Zwirnmann. Global effects of agriculture on fluvial dissolved organic matter. *Science Reports* 2015; **5**, 16328.
- [50] D Figueroa-Nieves, WH McDowell, JD Potter, G Martínez and JR Ortiz-Zayas. Effects of sewage effluents on water quality in tropical streams. *Journal of Environmental Quality* 2014; **43(6)**, 2053-2063.
- [51] MM Castillo. Land use and topography as predictors of nutrient levels in a tropical catchment. *Limnologica* 2010; **40(4)**, 322-329.
- [52] S Jiang, M Müller, J Jin, Y Wu, K Zhu, G Zhang, A Mujahid, T Rixen, MF Muhamad and ESA Sia. Dissolved inorganic nitrogen in a tropical estuary

- in Malaysia: Transport and transformation. *Biogeosciences* 2019; **16(14)**, 2821-2836.
- [53] W Xue, H Lhaetee, S Yu, T Jenkhetkan, B Hong, X Liu, P Chen, N Namngam and AS Tabucanon. Spatial and temporal variability of sedimentary nutrients in relation to regional development in the urbanizing lower Chao Phraya watersheds of Thailand. *Journal of Soils and Sediments* 2020; **20(11)**, 4042-4054.
- [54] SJ Goldberg, GI Ball, BC Allen, SG Schladow, AJ Simpson, H Masoom, R Soong, HD Graven and LI Aluwihare. Refractory dissolved organic nitrogen accumulation in high-elevation lakes. *Nature Communications* 2015; **6(1)**, 6347.
- [55] A Aruninta, H Matsushima and P Phukumchai. Flow or fence: Learning, preserving, and redefining the riverfront cultural landscape. *Journal of Water Resource and Protection* 2020; **12(11)**, 13.
- [56] S Ding, P Chen, S Liu, G Zhang, J Zhang and SF Dan. Nutrient dynamics in the Changjiang and retention effect in the Three Gorges Reservoir. *Journal of Hydrology* 2019; **574**, 96-109.
- [57] AE Khan, A Ireson, S Kovats, SK Mojumder, A Khusru, A Rahman and P Vineis. Drinking water salinity and maternal health in coastal bangladesh: Implications of climate change. *Environmental Health Perspectives* 2011; **119(9)**, 1328-1332.
- [58] M Ashrafuzzaman, C Artemi, FD Santos and L Schmidt. Current and future salinity intrusion in the south-western coastal region of Bangladesh. *Spanish Journal of Soil Science* 2022; **12**, 10017.
- [59] A Anukularmphai and A Rivas. A case study for interlinked coastal and river basin management for the bang Pakong River Basin, Available at: <https://doi.org/10.13140/RG.2.2.29230.92487>, accessed April 2025.
- [60] N Caraco and J Cole. Human impact on nitrate export: An analysis using major world rivers. *Ambio* 1999; **28**, 167-170.
- [61] SS Perakis and LO Hedin. Nitrogen loss from unpolluted South American forests mainly via dissolved organic compounds. *Nature* 2002; **415(6870)**, 416-419.
- [62] JJ Alberts and M Takács. Importance of humic substances for carbon and nitrogen transport into southeastern United States estuaries. *Organic Geochemistry* 1999; **30(6)**, 385-395.
- [63] AE Miller, JP Schimel, T Meixner, JO Sickman and JM Melack. Episodic rewetting enhances carbon and nitrogen release from chaparral soils. *Soil Biology and Biochemistry* 2005; **37(12)**, 2195-2204.
- [64] J Liu, G Han, X Liu, M Liu, C Song, Q Zhang, K Yang and X Li. Impacts of anthropogenic changes on the mun river water: Insight from spatio-distributions and relationship of C and N species in Northeast Thailand. *International Journal of Environmental Research and Public Health* 2019; **16(4)**, 659.
- [65] LA Martinelli, LD Coletta, EdC Ravagnani, PBd Camargo, JPHB Ometto, S Filoso and RL Victoria. Dissolved nitrogen in rivers: Comparing pristine and impacted regions of Brazil. *Brazilian Journal of Biology* 2010; **70**, 709-722.
- [66] L Wang, X Zhang, S Chen, F Meng, D Zhang, Y Liu, M Li, X Liu, X Huang and J Qu. Spatial variation of dissolved organic nitrogen in Wuhan surface waters: Correlation with the occurrence of disinfection byproducts during the COVID-19 pandemic. *Water Research* 2021; **198**, 117138.
- [67] J Wallace, L Stewart, A Hawdon, R Keen, F Karim and J Kemei. Flood water quality and marine sediment and nutrient loads from the Tully and Murray catchments in north Queensland, Australia. *Marine and Freshwater Research* 2009; **60(11)**, 1123-1131.
- [68] AC Tyler, KJ McGlathery and IC Anderson. Macroalgae mediation of dissolved organic nitrogen fluxes in a temperate coastal lagoon. *Estuarine, Coastal and Shelf Science* 2001; **53(2)**, 155-168.
- [69] J Laroche, R Nuzzi, R Waters, K Wyman, P Falkowski and D Wallace. Brown Tide blooms in Long Island's coastal waters linked to interannual variability in groundwater flow. *Global Change Biology* 1997; **3(5)**, 397-410.
- [70] Y Collos, C Jauzein, W Ratmaya, P Souchu, E Abadie and A Vaquer. Comparing diatom and Alexandrium catenella/tamarensis blooms in Thau lagoon: Importance of dissolved organic nitrogen in seasonally N-limited systems. *Harmful Algae* 2014; **37**, 84-91.

- [71] JB Crandall and MA Teece. Urea is a dynamic pool of bioavailable nitrogen in coral reefs. *Coral Reefs* 2012; **31(1)**, 207-214.
- [72] J Luang-on, J Ishizaka, A Buranapratheprat, J Phaksopa, JI Goes, H Kobayashi, M Hayashi, ER Maúre and S Matsumura. Seasonal and interannual variations of MODIS Aqua chlorophyll-a (2003 - 2017) in the Upper Gulf of Thailand influenced by Asian monsoons. *Journal of Oceanography* 2022; **78(4)**, 209-228.
- [73] GM Hallegraeff, ME Albinsson, J Dowdney, AK Holmes, MP Mansour and A Seger. Prey preference, environmental tolerances and ichthyotoxicity by the red-tide dinoflagellate *Noctiluca scintillans* cultured from Tasmanian waters. *Journal of Plankton Research* 2019; **41(4)**, 407-418.
- [74] SF Tsai, LY Wu, WC Chou and KP Chiang. The dynamics of a dominant dinoflagellate, *Noctiluca scintillans*, in the subtropical coastal waters of the Matsu archipelago. *Marine Pollution Bulletin* **127**, 553-558.
- [75] Coordinating Body on the Seas of East Asia. COBSEA strategic directions 2023 - 2027, Available at: <https://wedocs.unep.org/20.500.11822/44675>, accessed April 2025.

SPM	0.585**	0.165	0.398	1								
DSi	-0.595**	-0.130	-0.440*	-0.456*	1							
DIP	0.154	0.399	-0.141	0.19	0.165	1						
DIN	-0.304	0.172	-0.326	-0.186	0.462*	0.268	1					
NO ₃ ⁻	-0.578**	-0.462*	-0.286	-0.432*	0.156	-0.580**	0.126	1				
NO ₂ ⁻	-0.457*	-0.389	-0.175	-0.417*	0.199	-0.416*	0.031	0.712**	1			
NH ₄ ⁺	-0.029	0.369	-0.184	0.025	0.371	0.509*	0.903**	-0.305	-0.238	1		
DOP	0.451*	0.286	0.516*	0.128	-0.041	0.008	-0.195	-0.433*	-0.350	0.010	1	
DON	0.258	0.184	0.136	0.243	-0.082	0.765**	-0.239	-0.529*	-0.331	0.066	0.306	1
CPY												
Salinity	Salinity	pH	DO	SPM	DSi	DIP	DIN	NO ₃ ⁻	NO ₂ ⁻	NH ₄ ⁺	DOP	DON
Salinity	1											
pH	0.614**	1										
DO	0.742**	0.509*	1									
SPM	0.473*	0.338	0.300	1								
DSi	-0.306	-0.420*	-0.281	-0.077	1							
DIP	-0.216	0.213	-0.429*	-0.081	-0.202	1						
DIN	0.183	0.292	-0.099	0.406*	-0.185	0.556**	1					
NO ₃ ⁻	-0.755**	-0.389	-0.584**	-0.415*	-0.146	0.402	-0.203	1				
NO ₂ ⁻	0.178	0.247	-0.049	0.473*	-0.317	0.547**	0.855**	0.004	1			
NH ₄ ⁺	-0.135	0.022	-0.202	-0.076	0.325	0.142	0.408*	-0.309	-0.074	1		
DOP	-0.093	-0.137	-0.101	-0.074	0.407	-0.11	0.054	0.024	-0.059	0.313	1	
DON	-0.767**	-0.28	-0.655**	-0.340	0.193	0.516**	-0.081	0.845**	0.009	0.001	0.327	1
BPK												
Salinity	Salinity	pH	DO	SPM	DSi	DIP	DIN	NO ₃ ⁻	NO ₂ ⁻	NH ₄ ⁺	DOP	DON
Salinity	1											
pH	0.632**	1										
DO	-0.063	0.247	1									
SPM	0.453*	0.371	0.293	1								
DSi	-0.663**	-0.425*	-0.210	-0.353	1							
DIP	-0.133	-0.047	0.221	0.122	0.272	1						
DIN	-0.409*	0.03	0.233	-0.033	0.050	0.108	1					
NO ₃ ⁻	0.415*	0.167	-0.378	-0.117	-0.394	-0.179	-0.199	1				
NO ₂ ⁻	-0.379	0.075	0.306	0.022	0.089	0.174	0.971**	-0.319	1			
NH ₄ ⁺	-0.33	-0.409	-0.100	-0.246	0.225	-0.226	-0.252	-0.332	-0.381	1		
DOP	0.196	0.092	0.053	0.117	0.243	0.492*	-0.138	-0.088	-0.059	-0.193	1	
DON	0.221	0.128	-0.237	-0.328	0.095	0.136	0.062	0.118	0.142	-0.488*	0.268	1

** Correlation is significant at the 0.01 level (2-tailed).

* Correlation is significant at the 0.05 level (2-tailed).

Table S4 Pearson’s correlation from seasonal data (dry season).

MK												
Salinity	Salinity	pH	DO	SPM	DSi	DIP	DIN	NO ₃ ⁻	NO ₂ ⁻	NH ₄ ⁺	DOP	DON
Salinity	1											
pH	0.602*	1										
DO	-0.619**	-0.289	1									
SPM	0.691**	0.293	-0.595*	1								
DSi	-0.970**	-0.616**	0.591*	-0.733**	1							
DIP	-0.691**	-0.399	0.366	-0.633**	0.746**	1						
DIN	-0.973**	-0.567*	0.587*	-0.715**	0.970**	0.701**	1					
NO ₃ ⁻	-0.968**	-0.627**	0.618**	-0.717**	0.973**	0.672**	0.994**	1				
NO ₂ ⁻	-0.852**	-0.287	0.445	-0.774**	0.851**	0.716**	0.872**	0.837**	1			
NH ₄ ⁺	-0.341	0.293	-0.073	-0.169	0.276	0.461	0.365	0.258	-0.506*	1		
DOP	-0.147	-0.641**	0.015	0.002	0.184	0.143	0.104	0.144	-0.036	-0.269	1	
DON	0.492*	0.170	-0.417	0.405	-0.432	-0.119	-0.585*	-0.575*	-0.363	-0.306	0.02	1
TC												
Salinity	Salinity	pH	DO	SPM	DSi	DIP	DIN	NO ₃ ⁻	NO ₂ ⁻	NH ₄ ⁺	DOP	DON
Salinity	1											
pH	0.806**	1										
DO	0.691**	0.783**	1									
SPM	0.711**	0.598*	0.598*	1								
DSi	-0.973**	-0.763**	-0.676**	-0.837**	1							
DIP	-0.885**	-0.765**	-0.571*	-0.819**	0.905**	1						
DIN	-0.893**	-0.679**	-0.548*	-0.792**	0.930**	0.811**	1					
NO ₃ ⁻	-0.319	-0.054	0.067	-0.096	0.287	0.060	0.282	1				
NO ₂ ⁻	0.546*	0.620*	0.413	0.366	-0.533*	-0.448	-0.606*	-0.356	1			
NH ₄ ⁺	-0.890**	-0.683**	-0.553*	-0.794**	0.928**	0.814**	1.000**	0.258	-0.604*	1		
DOP	-0.719*	-0.376	-0.304	-0.617*	0.699*	0.442	0.705*	0.671*	-0.508	0.691*	1	
DON	-0.919**	-0.657**	-0.520*	-0.796**	0.942**	0.890**	0.863**	0.325	-0.343	0.859**	0.743**	1
CPY												
Salinity	Salinity	pH	DO	SPM	DSi	DIP	DIN	NO ₃ ⁻	NO ₂ ⁻	NH ₄ ⁺	DOP	DON
Salinity	1											
pH	0.341	1										
DO	0.308	0.770**	1									
SPM	0.626**	-0.056	-0.085	1								
DSi	0.809**	0.121	0.088	0.863**	1							
DIP	-0.882**	-0.530*	-0.552*	-0.475	-0.684**	1						
DIN	-0.934**	-0.406	-0.388	-0.598*	-0.745**	0.911**	1					
NO ₃ ⁻	-0.890**	-0.519*	-0.376	-0.557*	-0.699**	0.827**	0.961**	1				

NO ₂ ⁻	-0.942**	-0.347	-0.379	-0.694**	-0.830**	0.916**	0.964**	0.890**	1			
NH ₄ ⁺	-0.861**	-0.249	-0.360	-0.506*	-0.647**	0.904**	0.945**	0.830**	0.909**	1		
DOP	-0.084	0.022	0.285	-0.066	-0.009	-0.222	0.159	0.338	0.020	-0.012	1	
DON	-0.848**	-0.501*	-0.381	-0.484*	-0.622**	0.758**	0.884**	0.939**	0.793**	0.755**	0.361	1

BPK

Salinity	Salinity	pH	DO	SPM	DSi	DIP	DIN	NO ₃ ⁻	NO ₂ ⁻	NH ₄ ⁺	DOP	DON
Salinity	1											
pH	0.707**	1										
DO	0.922**	0.665**	1									
SPM	0.714**	0.591*	0.582*	1								
DSi	-0.992**	-0.669**	-0.907**	-0.684**	1							
DIP	-0.912**	-0.623*	-0.876**	-0.680**	0.926**	1						
DIN	-0.958**	-0.694**	-0.854**	-0.798**	0.952**	0.940**	1					
NO ₃ ⁻	-0.946**	-0.623*	-0.832**	-0.740**	0.948**	0.915**	0.977**	1				
NO ₂ ⁻	0.775**	0.367	0.655**	0.491	-0.793**	-0.724**	-0.777**	-0.892**	1			
NH ₄ ⁺	0.700**	0.683**	0.649**	0.757**	-0.693**	-0.653**	-0.773**	-0.735**	0.511	1		
DOP	-0.078	-0.044	-0.024	-0.312	0.051	0.144	0.147	0.043	0.170	-0.014	1	
DON	-0.399	-0.530*	-0.198	-0.474	0.368	0.337	0.468	0.492	-0.477	-0.225	0.239	1

** Correlation is significant at the 0.01 level (2-tailed).

* Correlation is significant at the 0.05 level (2-tailed).

Table S5 Pearson’s correlation from seasonal data (wet season).

MK

Salinity	Salinity	pH	DO	SPM	DSi	DIP	DIN	NO ₃ ⁻	NO ₂ ⁻	NH ₄ ⁺	DOP	DON
Salinity	1											
pH	-0.328	1										
DO	-0.893**	0.189	1									
SPM	0.549**	0.159	-0.709**	1								
DSi	-0.777**	0.254	0.604**	-0.413	1							
DIP	-0.793**	0.343	0.656**	-0.305	0.700**	1						
DIN	-0.741**	0.481*	0.614**	-0.401	0.758**	0.684**	1					
NO ₃ ⁻	-0.845**	0.313	0.707**	-0.475*	0.905**	0.773**	0.841**	1				
NO ₂ ⁻	-0.833**	0.274	0.748**	-0.571**	0.883**	0.686**	0.818**	0.914**	1			
NH ₄ ⁺	0.160	0.313	-0.15	0.130	-0.237	-0.131	0.313	-0.251	-0.157	1		
DOP	0.506*	-0.020	-0.384	0.231	-0.456*	-0.579**	-0.456*	-0.616**	-0.438*	0.252	1	
DON	0.261	-0.421	-0.076	-0.055	-0.403	-0.143	-0.679**	-0.397	-0.386	-0.525*	0.065	1

TC

Salinity	Salinity	pH	DO	SPM	DSi	DIP	DIN	NO ₃ ⁻	NO ₂ ⁻	NH ₄ ⁺	DOP	DON
Salinity	1											
pH	-0.302	1										
DO	0.563*	-0.033	1									
SPM	0.913**	-0.333	0.454	1								
DSi	-0.987**	0.33	-0.610*	-0.934**	1							
DIP	-0.971**	0.395	-0.632**	-0.915**	0.990**	1						
DIN	-0.952**	0.197	-0.627**	-0.872**	0.961**	0.931**	1					
NO ₃ ⁻	-0.382	0.242	0.025	-0.471	0.29	0.216	0.298	1				
NO ₂ ⁻	0.826**	-0.145	0.670**	0.796**	-0.812**	-0.768**	-0.831**	-0.699*	1			
NH ₄ ⁺	-0.952**	0.198	-0.629**	-0.871**	0.960**	0.931**	1.000**	0.290	-0.834**	1		
DOP	-0.722**	0.274	-0.435	-0.751**	0.700**	0.679**	0.583**	0.398	-0.709**	0.581*	1	
DON	-0.327	0.431	-0.222	-0.372	0.327	0.372	0.091	0.268	-0.284	0.091	0.737**	1

CPY

Salinity	Salinity	pH	DO	SPM	DSi	DIP	DIN	NO ₃ ⁻	NO ₂ ⁻	NH ₄ ⁺	DOP	DON
Salinity	1											
pH	0.347	1										
DO	-0.493*	-0.054	1									
SPM	0.379	0.697**	-0.192	1								
DSi	-0.829**	-0.615**	0.218	-0.725**	1							
DIP	-0.642**	-0.766**	0.197	-0.775**	0.894**	1						
DIN	-0.815**	-0.599**	0.255	-0.714**	0.978**	0.871**	1					
NO ₃ ⁻	-0.721**	-0.534**	0.200	-0.653**	0.919**	0.824**	0.949**	1				
NO ₂ ⁻	-0.753**	-0.734**	0.246	-0.764**	0.943**	0.941**	0.952**	0.904**	1			
NH ₄ ⁺	-0.833**	-0.583**	0.270	-0.703**	0.970**	0.847**	0.990**	0.898**	0.929**	1		
DOP	-0.521*	-0.404	0.166	-0.644**	0.735**	0.656**	0.771**	0.859**	0.725**	0.710**	1	
DON	-0.722**	-0.599**	0.159	-0.636**	0.922**	0.861**	0.952**	0.977**	0.926**	0.908**	0.863**	1

BPK

Salinity	Salinity	pH	DO	SPM	DSi	DIP	DIN	NO ₃ ⁻	NO ₂ ⁻	NH ₄ ⁺	DOP	DON
Salinity	1											
pH	0.924**	1										
DO	0.757**	0.917**	1									
SPM	0.562*	0.648**	0.575*	1								
DSi	-0.954**	-0.912**	-0.825**	-0.574*	1							
DIP	-0.888**	-0.956**	-0.893**	-0.713**	0.880**	1						
DIN	-0.894**	-0.961**	-0.849**	-0.736**	0.869**	0.967**	1					
NO ₃ ⁻	-0.937**	-0.862**	-0.734**	-0.571*	0.921**	0.787**	0.815**	1				
NO ₂ ⁻	-0.969**	-0.937**	-0.845**	-0.609*	0.992**	0.910**	0.907**	0.939**	1			
NH ₄ ⁺	-0.753**	-0.881**	-0.789**	-0.722**	0.722**	0.925**	0.959**	0.618*	0.767**	1		
DOP	0.079	0.127	0.238	-0.449	-0.149	-0.098	-0.060	-0.051	-0.15	-0.050	1	
DON	0.344	0.447	0.378	0.253	-0.349	-0.479	-0.549*	-0.200	-0.372	-0.648**	0.401	1

** Correlation is significant at the 0.01 level (2-tailed).

* Correlation is significant at the 0.05 level (2-tailed).

Supplementary section 2: In-depth description

Physicochemical parameters distribution

Physical and chemical parameters exhibited distinct spatial and seasonal variability across the study area (**Figure S1**). Surface water temperatures ranged from 24.9 - 34.9 °C, with higher values generally recorded during the dry season (> 30 °C) and lower values in the wet season (< 30 °C), likely influenced by increased cloud cover and rainfall. Salinity varied markedly from near 0 at upstream stations to approximately 29.0 at downstream stations, reflecting strong riverine freshwater input and seawater intrusion from the GoT, with the highest salinity observed at the BPK downstream station during the wet season. pH values ranged narrowly (6.75 - 8.31) and showed minimal spatial or seasonal variability, though upstream stations had slightly lower average pH (7.59 ± 0.27) than downstream ones (7.73 ± 0.22). An exception was BPK, where pH was lower in the dry season (7.82 ± 0.073) than in the wet season (8.04 ± 0.137). DO concentrations also lacked a consistent seasonal pattern but tended to be lower at upstream stations ($3.05 \pm 1.93 \text{ mg L}^{-1}$) compared to downstream stations ($3.74 \pm 1.70 \text{ mg L}^{-1}$), except at MK, where DO was higher in the dry season. Critically low DO levels (< 2.0 mg L^{-1}) were observed at the downstream stations of TC-1 and CPY-1. SPM exhibited substantial spatial and seasonal variation, with significantly higher concentrations during the dry season ($140 \pm 172 \text{ mg L}^{-1}$) than in the wet season ($45.6 \pm 52.0 \text{ mg L}^{-1}$), and elevated levels at downstream stations ($90.2 \pm 126.0 \text{ mg L}^{-1}$) compared to upstream stations ($26.5 \pm 25.0 \text{ mg L}^{-1}$) ($p < 0.05$), indicating sediment resuspension and reduced dilution during drier periods.

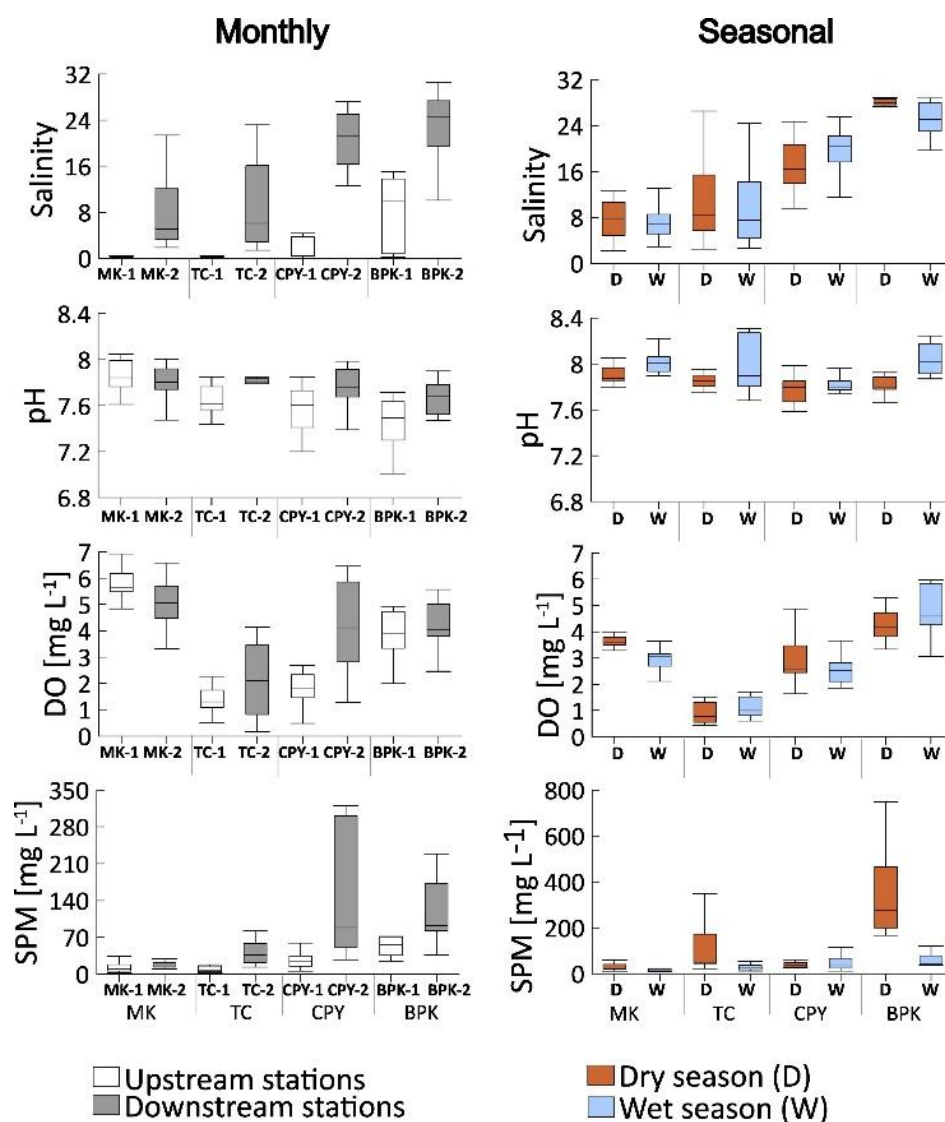


Figure S1 Box plots of physicochemical parameters and nutrients across the four river basins, categorized by monthly (Upstream-Downstream stations) and seasonal (Dry-Wet season).

Spatial nutrient distribution

Nutrient concentrations along the four main rivers varied greatly in both space and time (**Figure 3**). DSi in the main rivers ranged from 5.53 to 270 μM . It was relatively higher at the upstream stations ($156 \pm 65.8 \mu\text{M}$) than at the downstream stations ($132 \pm 63.6 \mu\text{M}$), reflecting riverine inputs. Among rivers, the TC exhibited the highest average DSi concentration at both upstream ($205 \pm 51.0 \mu\text{M}$) and downstream stations ($177 \pm 66.6 \mu\text{M}$).

DIP concentrations showed no consistent trend between upstream and downstream stations, ranging from not detected (nd), below detection limits, to 23.3 μM . Only the TC basin exhibited a significant difference between upstream and downstream ($p < 0.05$), with average DIP concentrations of 4.34 ± 0.77 and $11.0 \pm 5.74 \mu\text{M}$ at the upstream and downstream stations, respectively.

DIN species (NO_3^- , NO_2^- , and NH_4^+) exhibited distinct spatial patterns throughout the rivers. Average DIN was relatively higher at the upstream stations ($51.8 \pm 27.0 \mu\text{M}$) compared to the downstream stations ($45.3 \pm 32.0 \mu\text{M}$), except for the CPY River. In general, NO_3^- concentrations in the four main rivers ranged from nd to 230 μM . NO_3^- was significantly higher at the upstream stations ($62.3 \pm 54.8 \mu\text{M}$) compared to the downstream stations ($17.0 \pm 17.9 \mu\text{M}$), particularly evident at the CPY and BPK Rivers.

NO_2^- , as an intermediate species, showed no clear upstream–downstream trend. The CPY River recorded the highest average concentration ($\sim 30 \mu\text{M}$), while the MK River had the lowest ($\sim 1 \mu\text{M}$). In the CPY and MK rivers, upstream NO_2^- concentrations were approximately 7 and 2 times higher than downstream concentrations, respectively. NH_4^+ levels were generally similar across locations, except at TC, where upstream concentrations were roughly half those downstream. The highest average NH_4^+ ($55.0 \pm 50.1 \mu\text{M}$) was observed at the downstream station (TC-2).

Dissolved organic nutrients (DOP and DON) differed in distribution from inorganic forms. DOP concentration (0.01 - 11.2 μM) was lower than DIP (1.04 - 23.3 μM) but followed a similar spatial pattern, with the highest average at TC-2 ($2.93 \pm 2.88 \mu\text{M}$). In contrast, DON showed a broader range (0.13 - 304 μM) than DIN (10.3 - 174 μM) and exhibited distinct spatial variation. At CPY, the DON average was twice as high upstream (CPY-1) as downstream (CPY-2), whereas DIN levels were similar. At TC, the DON median was lower upstream than downstream, opposite to the DIN pattern. Similar to DIN, MK showed the lowest DON concentrations.

For the seasonal data (**Figure 3**), median and distribution values were calculated from all water column layers at each river mouth. DSi averages were lower in the dry season ($112 \pm 60.1 \mu\text{M}$) than in the wet season ($158 \pm 74.3 \mu\text{M}$). MK ($160 \pm 27.4 \mu\text{M}$ in dry season and $208 \pm 16.4 \mu\text{M}$ in wet season, respectively) and TC (168 ± 51.6 and $222 \pm 46.1 \mu\text{M}$, respectively) showed the highest averages, while BPK (52.9 ± 17.5 and $39.3 \pm 19.0 \mu\text{M}$, respectively) showed the lowest in both periods.

DIP averages in the dry season were lower at MK and TC but higher at CPY and BPK. TC consistently exhibited the highest DIP average across both dry and wet seasons (8.88 ± 39.0 and $12.5 \pm 3.55 \mu\text{M}$, respectively). DIN showed a similar pattern, with dry season averages being lower at MK and TC, and higher at CPY and BPK. The highest DIN average occurred at TC in the wet season ($122 \pm 31.5 \mu\text{M}$), followed by CPY in the dry season ($86.9 \pm 22.2 \mu\text{M}$). NO_3^- averages were generally higher in the dry season ($25.3 \pm 19.4 \mu\text{M}$) than in the wet season ($14.1 \pm 11.5 \mu\text{M}$), except at MK. TC had the lowest NO_3^- values (1.38 ± 0.25 and $0.54 \pm 0.33 \mu\text{M}$, respectively), near 0. NO_3^- averages in the dry season at CPY ($36.3 \pm 10.2 \mu\text{M}$) and BPK ($44.0 \pm 18.6 \mu\text{M}$) were the highest. NO_2^- in the dry season followed a similar spatial pattern, with lower concentrations at MK and TC, and higher at CPY and BPK. NH_4^+ averages increased from the dry season ($10.7 \pm 10.6 \mu\text{M}$) to the wet season ($43.6 \pm 44.4 \mu\text{M}$) at all river mouths. TC had the highest NH_4^+ average in the wet season ($120 \pm 31.7 \mu\text{M}$).

DOP averages remained similar between sampling periods at most sites, except at CPY, where the average from the dry season ($1.32 \pm 0.384 \mu\text{M}$) was approximately three times lower than the wet season ($4.64 \pm 0.800 \mu\text{M}$). DON concentrations were generally low ($\sim 20 \mu\text{M}$) at MK and BPK in both periods. However, the DON average from the dry season at CPY was also three times lower than BPK, mirroring the DOP pattern.

Vertical profile of physicochemical parameters distribution

Figure S2 presents the vertical gradients of physicochemical parameters at the river mouths during the dry and wet seasons. Salinity gradients revealed distinct estuarine classifications. MK exhibited a stratified estuary structure, characterized by bottom-layer seawater intrusion in both seasons. TC and BPK showed uniform salinity profiles, classifying them as well-mixed estuaries [1]. CPY exhibited slight bottom-layer seawater intrusion, indicating a partially mixed estuary. Salinity at MK was higher in the dry season (~ 22.5) than in the wet season (~ 12.5). At TC, seawater intrusion (salinity ~ 25) extended further inland in the wet season than in the dry season. CPY and BPK exhibited similar salinity levels and distributions across both seasons.

pH gradients did not consistently correlate with salinity patterns. At MK, pH was lower in the dry season (7.90 ± 0.070) than in the wet season (8.01 ± 0.089). At TC, mean pH values were similar between seasons (dry: 7.89 ± 0.121 ; wet: 7.97 ± 0.224), but spatial distributions varied. In the dry season, seawater masses exhibited higher pH (~ 8.2) than brackish waters (~ 7.8), whereas in the wet season, elevated pH (~ 8.3) was observed at TC-2 and TC-4. CPY had comparable mean pH values across seasons (dry: 7.97 ± 0.130 ; wet: 7.82 ± 0.066), though pH near 0 km was slightly higher in the dry season. At BPK, dry season pH (7.82 ± 0.073) was lower than in the wet season (8.04 ± 0.137), with a noticeable seaward increase during the wet season (from ~ 7.9 at BPK-2 to 8.2 at BPK-7).

DO concentrations were generally elevated at the surface, particularly at MK and CPY during the wet season, and often peaked at the interface of saline and freshwater masses, notably at TC, CPY, and BPK. DO patterns differed seasonally at MK and CPY but were relatively consistent at TC and BPK. At MK, DO levels were uniform ($\sim 3.5 \text{ mg L}^{-1}$) in the dry season, but higher near the surface during the wet season. At TC, elevated DO was consistently observed at the offshore station (TC-8). At CPY, higher DO ($4 - 5 \text{ mg L}^{-1}$) in the dry season began upstream at CPY-5. Mean DO was greater in the dry season ($3.04 \pm 1.02 \text{ mg L}^{-1}$) than in the wet season ($2.06 \pm 0.580 \text{ mg L}^{-1}$), where surface values ($\sim 3.5 \text{ mg L}^{-1}$) were dominant. At BPK, DO increased seaward in both seasons, with slightly lower average levels in the dry season ($4.26 \pm 0.633 \text{ mg L}^{-1}$) compared to the wet season ($4.78 \pm 0.952 \text{ mg L}^{-1}$).

SPM was generally higher in bottom waters, particularly at MK and BPK during the dry season, and also peaked at salinity interfaces, especially at TC. At MK, bottom-layer SPM concentrations ($\sim 300 \text{ mg L}^{-1}$) were prominent in the dry season (MK-5), whereas the wet season showed lower, more homogeneous values ($30.9 \pm 42.1 \text{ mg L}^{-1}$). At TC, SPM peaked at the offshore station (TC-8) during the dry season ($\sim 400 \text{ mg L}^{-1}$); mean concentrations were significantly higher in the dry season ($129 \pm 135 \text{ mg L}^{-1}$) compared to the wet season ($31.0 \pm 20.0 \text{ mg L}^{-1}$). At CPY, SPM levels were consistent across seasons, with high bottom concentrations ($\sim 150 \text{ mg L}^{-1}$) at CPY-3 (dry) and CPY-2 (wet). Mean values were $46.7 \pm 37.8 \text{ mg L}^{-1}$ (dry) and $61.4 \pm 79.7 \text{ mg L}^{-1}$ (wet). BPK showed the highest dry season SPM ($\sim 750 \text{ mg L}^{-1}$) between BPK-4 and BPK-5, with an average of $358 \pm 192 \text{ mg L}^{-1}$; wet season levels were much lower ($59.6 \pm 29.1 \text{ mg L}^{-1}$), with a seaward increase from $\sim 50 \text{ mg L}^{-1}$ (BPK-2) to 120 mg L^{-1} (BPK-7).

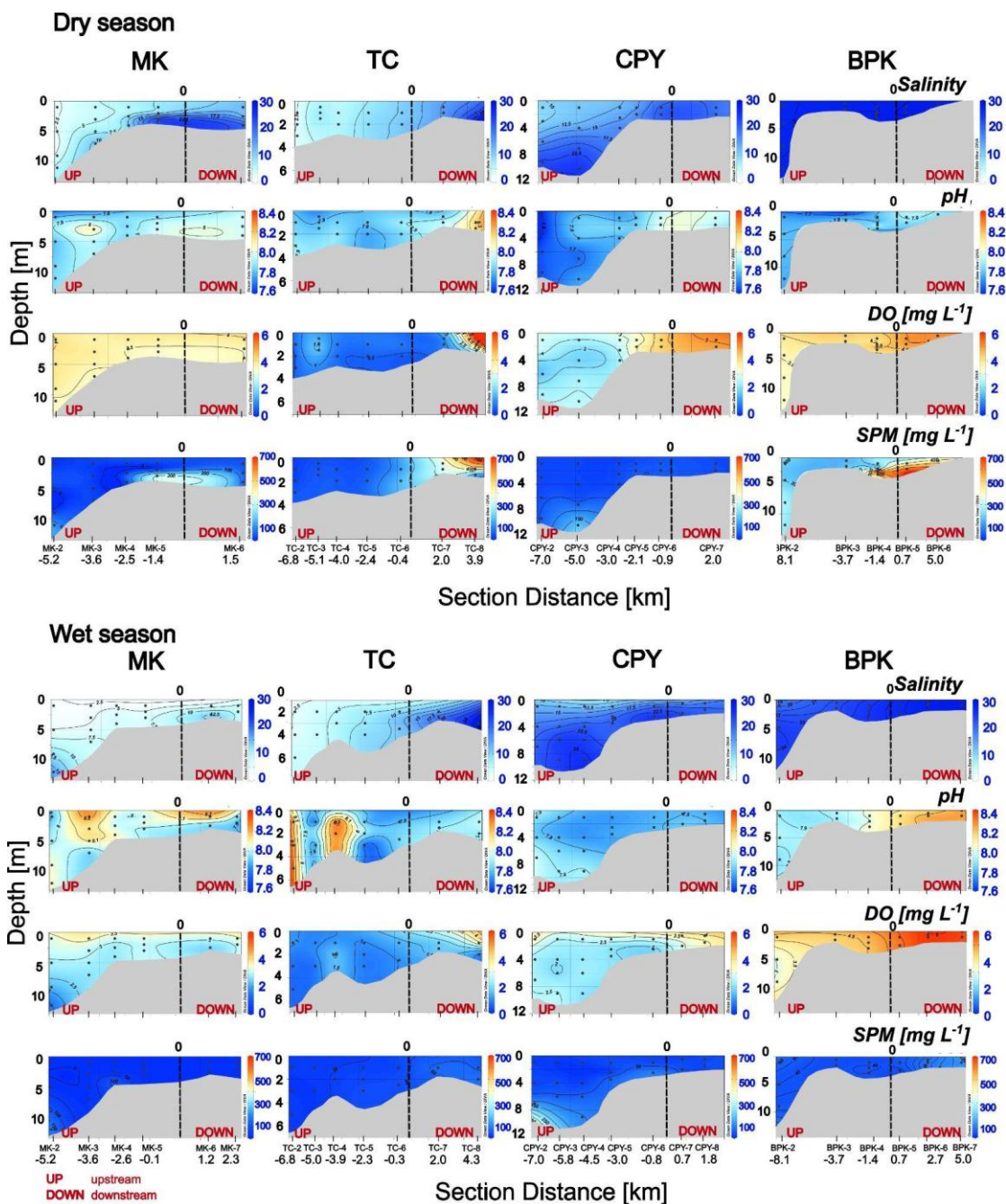


Figure S2 The vertical profiles of physicochemical parameters in the dry and wet seasons are presented. The parameters include salinity, pH, DO, and SPM. In each figure, the vertical dashed line represents the coastline at the river mouth. The 0 km mark on the x-axis represents the innermost stations at the river mouth, corresponding to the monthly sampling locations.

Vertical profile of nutrient distribution

The distribution of DS_i generally followed the salinity gradient, with higher concentrations in low-salinity waters and lower concentrations in high-salinity areas. In all river mouths, DS_i concentrations were higher in the wet season than in the dry season, except at BPK, where levels were comparable between seasons (dry: 52.9 ± 17.5 μM; wet: 39.3 ± 19.0 μM). At CPY, DS_i distribution in the dry season did not clearly follow the salinity gradient and exhibited a lower average concentration (66.6 ± 4.62 μM) compared to the wet season (145 ± 33.9 μM).

DIP also tended to follow salinity gradients, although less clearly than DS_i. For instance, at MK during the wet season, DIP distribution did not align closely with the salinity contours. DIN in the dry season generally corresponded

with salinity gradients, with higher concentrations in low-salinity waters at MK and CPY. Although DIN tended to increase seaward, its contours did not clearly align with salinity. In the wet season, DIN distributions were less consistent with salinity gradients; however, elevated DIN concentrations in low-salinity waters were observed across all river mouths.

Each dissolved inorganic nitrogen (DIN) species exhibited distinct spatial distributions across river mouths (**Figures 4 and 5**). Some species followed salinity gradients, while others did not. During the dry season, NO_3^- concentrations were generally higher in low-salinity waters across all river mouths, except at TC, where the distribution was patchy and the average concentration was lowest ($1.38 \pm 0.25 \mu\text{M}$). In the wet season, NO_3^- concentrations were more uniform throughout the water column and did not clearly correlate with salinity.

NO_2^- distribution in the dry season at MK and CPY followed the salinity gradient, with elevated concentrations in low-salinity waters. At TC, NO_2^- levels were low and showed no clear pattern, while at BPK, concentrations were lower in low-salinity waters, opposing the expected trend. In the wet season, NO_2^- distributions did not align with salinity patterns. At MK and CPY, surface waters had higher NO_2^- concentrations than bottom waters. TC showed an increasing trend seaward, while BPK displayed a decreasing seaward gradient.

NH_4^+ distributions were site-specific but relatively consistent across seasons. At MK, concentrations were low and showed no clear relationship with salinity. At TC, although unrelated to salinity, NH_4^+ concentrations decreased seaward. At CPY, NH_4^+ distribution closely followed the salinity gradient, with higher concentrations in low-salinity waters. At BPK, NH_4^+ levels did not correspond with salinity in either season; concentrations were very low in the dry season but showed a decreasing seaward trend during the wet season.

The distribution of dissolved organic species was generally non-uniform and did not consistently follow salinity gradients. At MK, DOP concentrations remained low ($\sim 1 \mu\text{M}$) throughout the water column in both seasons, with no distinct concentration hotspots. At TC, DOP was higher ($\sim 2 \mu\text{M}$), with a notable peak ($\sim 5 \mu\text{M}$) at the mid-depth of TC-2 during the dry season. In the dry season at CPY, DOP was slightly lower at the mid-layer of CPY-3 ($\sim 0.4 \mu\text{M}$), while the overall average was $1.32 \pm 0.384 \mu\text{M}$. In the wet season, a high DOP concentration was observed in the surface layer between CPY-2 and CPY-3. At BPK, DOP remained consistently low ($\sim 1 \mu\text{M}$) in both seasons, with no clear spatial variability.

DON at MK was uniform in both seasons, showing no notable vertical or horizontal variation. At TC, DON concentrations were high in the dry season ($77.3 \pm 33.8 \mu\text{M}$), decreasing seaward to $\sim 25 \mu\text{M}$. In the wet season, localized peaks were observed at the bottom of TC-2 and the surface of TC-5, while a low concentration zone appeared at the bottom of TC-5. CPY was the only site where DON distribution followed the salinity gradient. In the dry season, lower DON concentrations ($\sim 40 \mu\text{M}$) were found at the bottom of CPY-3, CPY-6, and CPY-7 within high-salinity waters, with an overall average of $53.7 \pm 19.6 \mu\text{M}$. In the wet season, elevated DON concentrations were observed in surface layers associated with low salinity. At BPK, dry season DON peaked ($\sim 40 \mu\text{M}$) at the surface between BPK-2 and BPK-3, whereas in the wet season, a low concentration zone ($\sim 15 \mu\text{M}$) was present at the bottom layer in the same area.

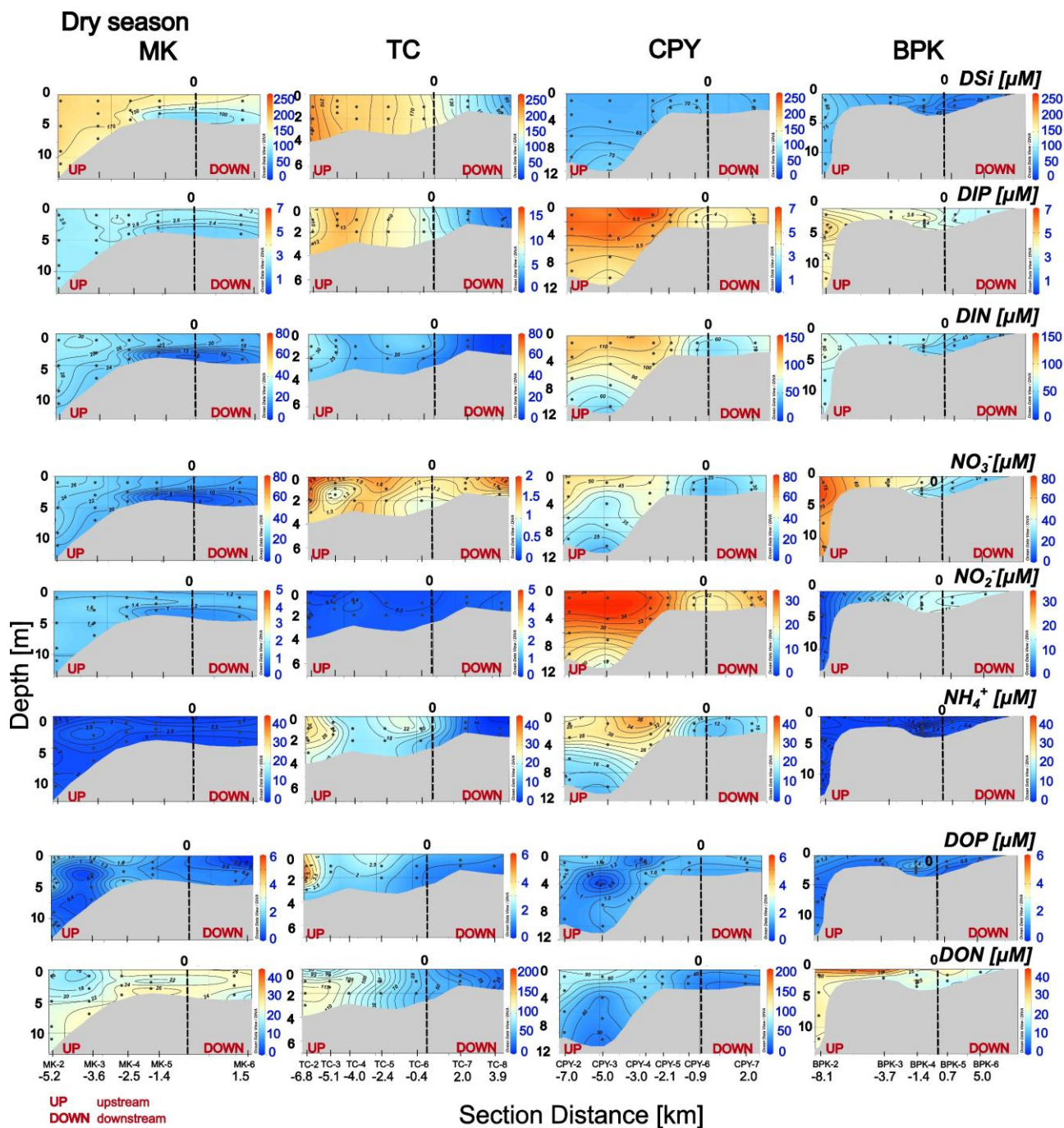


Figure S3 The vertical profiles of inorganic nutrients in the dry seasons are presented. The parameters include dissolved silicate (DSi), dissolved inorganic phosphate (DIP), dissolved inorganic nitrogen (DIN), nitrate (NO_3^-), nitrite (NO_2^-), ammonia (NH_4^+), dissolved organic phosphorus (DOP) and dissolved organic nitrogen (DON). In each figure, the vertical dashed line represents the coastline at the river mouth. The 0 km mark on the x-axis represents the innermost stations at the river mouth, corresponding to the monthly sampling locations.

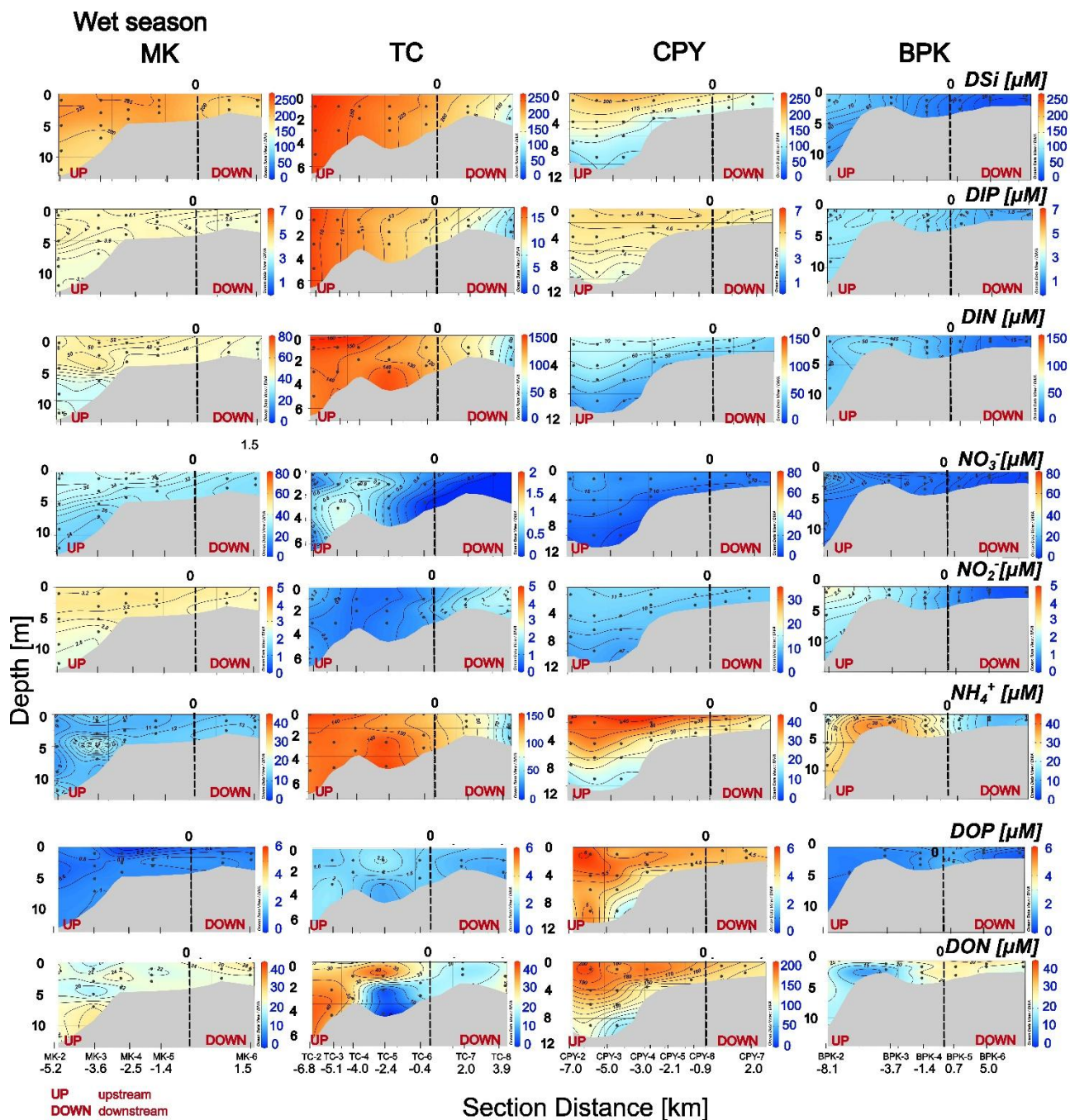


Figure S4 The vertical profiles of inorganic nutrients in the wet seasons are presented. The parameters include dissolved silicate (DSi), dissolved inorganic phosphate (DIP), dissolved inorganic nitrogen (DIN), nitrate (NO_3^-), nitrite (NO_2^-), ammonia (NH_4^+), dissolved organic phosphorus (DOP) and dissolved organic nitrogen (DON). In each figure, the vertical dashed line represents the coastline at the river mouth. The 0 km mark on the x-axis represents the innermost stations at the river mouth, corresponding to the monthly sampling locations.